Journal of Applied Sciences and Nanotechnology

Journal homepage: jasn.uotechnology.edu.iq

Advanced Photovoltaic Applications of CdO Films Prepared by Pulsed Laser Ablation on Porous Silicon

[1]Raghad R. Mahdi, [2]Marwa Kasim Abood*

[1]Energy and Renewable Energies Technology Center, University of Technology-Iraq, Baghdad, Iraq
[2]Department of Applied Sciences, University of Technology-Iraq, Iraq

A R T I C L E I N F O

Article history:
Received: April, 21, 2024
Accepted: September, 01, 2024
Available online: September, 10, 2024

Keywords:
Pulsed laser ablation,
Cadmium oxide,
Solar cell,
Porous silicon

Corresponding Author:
Marwa Kasim Abood
marwa.k.abood@uotechnology.edu.iq

A B S T R A C T

In this study, cadmium oxide (CdO) was prepared by pulsed laser ablation in liquid (PLAL). The morphological structure and optical properties of the prepared CdO were determined by various analytical techniques, including SEM, AFM and XRD. The SEM images obtained showed that the prepared film exhibited cluster-like cubic structures. The AFM images showed a homogeneous and very uniform surface. In addition, XRD analysis revealed that the prepared film had a grain size of about 20 nm. The optical properties of the fabricated film showed an increase in absorbance values with a simultaneous increase in wavelength. The maximum value was measured at 340 nm, and the measured optical energy gap was about 2.55 electron volts (eV). The solar cell was produced by depositing a CdO film on the porous silicon. The fabricated solar cell achieved an efficiency of 0.16%. Therefore, the CdO film from this work could be an important factor for the development of gas sensors and solar cells. In addition, other powerful analytical techniques were performed in this study, including X-ray diffraction (XRD), Fourier transform infrared spectroscopy (FTIR) and photoluminescence (PL) observations.

https://doi.org/10.53293/jasn.2024.7353.1286, Department of Applied Sciences, University of Technology - Iraq.
© 2024 The Author(s). This is an open access article under the CC BY license (http://creativecommons.org/licenses/by/4.0/).

1. Introduction

Cadmium oxide (CdO) has aroused great interest in the scientific community due to its unique properties. CdO occurs in nature; its band gap energy ranges from 2.1 to 6.2 eV, depending on the preparation conditions, its high density of 8150 kg /m^3 and its solubility in water. CdO, one of the most important novel materials in solar cell technology, can increase photoelectric conversion efficiency. CdO is a semiconductor material with unique electrical properties that play a crucial role in solar cells, such as improving efficiency. It is also used as a transparent conducting oxide (TCO) layer. CdO is a promising TCO like window glasses with dual functions, which allows the light to go through because transparency is necessary to maximize light absorption, thus ultimately enabling semiconductor layers to convert light to electricity. It also facilitates electric charge movement inside the device. CdO may also serve as a buffer coat layer in specific solar cells by controlling the bonding of various semiconducting materials, which, consequently, reduces the error rate and increases the device's stability [1-9]. The thinnest film structure of CdO is a nanoscale version coated onto different substrates to serve various purposes, such as Atomic Layer Deposition, Spray Pyrolysis, Sol-gel method, Chemical Vapor Deposition (CVD),

and Sputtering. ALD is suitable for the precise and controlled in situ deposition of atomic layers using gas-phase precursors. Volatile precursors undergo chemical reactions that are a part of the CVD process. Sputtering is a process that takes ions of high energy from a target material and releases atoms. The resulting spray pyrolysis atomizes the Cd-based salt solution. This method involves the spin-coating, dip-coating, or Sol-Gel Method onto a substrate [10, 11].

In the Pulsed Laser Ablation (PLA) method, short pulses of laser light beam are utilized to remove or ablate the targeted material from the surface. PLA is a promising method in several science fields, such as materials science, nanotechnology, and medicine. Powerful laser pulses are generated precisely and progressively using the PLA technique, which involves directing a target and removing material from its surface. The substance is rapidly heated and vaporized due to interaction with the powerful and directed laser beams. As a result, the material is removed as a plasma plume. PLA contributes to nanoparticle synthesis, which is vital in nanotechnology. The ablation process can control the sizes and compositions of the synthesized nanoparticles. These nanoparticles are used in materials improvement, imaging, and medication delivery systems [12, 13]. The advantages of employing pulsed laser ablation in liquid include its ability to offer high precision and control in the deposition of thin films. Thermal Evaporation was used to depose CdO films for precise configuration of thickness, structure, and uniformity on the atomic level. Employing liquid–pulsed laser ablation–facilitates CdO nanoparticle production by targeting high-purity CdO [14]. In addition, the interconnection between CdO films and porous silicon (PSi) contributes to creating innovative methods to improve light absorption and charge collection in solar cells. PSi contains a high surface area and light-trapping effects, providing a robust scaffold for CdO film treatment. Especially in silicon material the porous structure is positioned appropriately to increase photon intake and more efficient photon energy utilization. CdO film has been deposited on the PSi substrate to combine the electrical properties of CdO with the light absorption capabilities of PSi. As a result, higher device performance will improve [15].

The present research aims to develop a new technology for producing solar cells, contributing to advancing renewable energy technology and photonic applications. Also, this is the first study that proposed the design and analysis of CdO film fabrication, along with their integration with porous silicon layers, which will be used as sensors in solar cell applications. However, the CdO films have been studied for various optoelectronic applications; the method in this study is distinguished from previous techniques with its certain unique features. The research sheds light on the unique aspects of the proposed approach and its applications compared with previously studied methods. Thus, the results are suggested to be the basis for the future development of CdO film synthesis and its applications in solar cells. Implementing a multi-component approach, particularly incorporating pulsed laser ablation in liquid, PSi integration, and advanced characterization techniques, might be the most promising strategy for developing high-performance CdO-based solar.

2. Experimental Procedure

2.1 Material

A 10 g of CdO coarse powder was manually prepared using a special grinder. The prepared material was sieved with a regular 38-micrometer sieve. The resulting fine powder was compressed into a tablet with a 12 mm diameter. This CdO tablet was subsequently immersed in 50 mL of deionized distilled water. The PLA process used the 532 nm wavelength Q-switching (Nd: YAG) laser. The CdO tablet is bombarded with energy of 480 mJ with 200 pulses; the pulse duration at 15 ns, and the frequency of laser pulses was 3 Hz.

2.2 Sample Preparation

A PSi substrate was prepared via the electrochemical method by mixing a 1.5×1 cm well-cleaned (p-type) silicon wafer with a solution of HF and ethanol for 3 minutes. The selected etching parameters were a high concentration solution of 40% HF and ethanol 99.99% at room temperature, with a current density of 18 mL/cm^2 and an etching time of 15 s to obtain silicon with a homogenous porosity distribution and appropriate size pores on the surface. A drop casting method was used to deposit CdO nanoparticles on the PSi special syringe, where five drops are gradually dripped until the material dries on the porous silicon. A solar cell is fabricated by depositing Al film to achieve ohmic contact on the Al/CdO/ PSi /Si/Al structure.

2.3 Characterization

The analyzed optical properties of CdO film deposited on quartz substrates. The films absorption spectra were measured using a spectral photometer (1800 UV-visible spectrometer) in a range between 300 to1100 nm. The energy band gap (Eg), Extinction coefficient (K), and optical conductivity (σ) were measured using equations of [14]. The structural properties of the prepared film were investigated using an x-ray diffractometer (Shimadzu 6000), and the grain size D, density of dislocation δ, and strain ε were extracted using the equations listed in the literature [15]. Many other optical constants related to the fabricated cell were also measured, such as (I-V) characteristics in dark and illuminated conditions in a forward and reverse bias and solar cell characters such as Im, Vm, Ics, Voc and filling factor (FF) to measure the conversion efficiency of the fabricated cell.

3. Result and Discussion

The topographic characteristics of the CdO film results were analyzed by SEM images, as shown in **Fig. 1**. The SEM images showed that the deposited CdO particles on the PSi surface appeared in different sizes. The largest CdO particles are likely in cubic form, while the smallest is in cluster form, consisting of various particle sizes diffused within the porous structure.

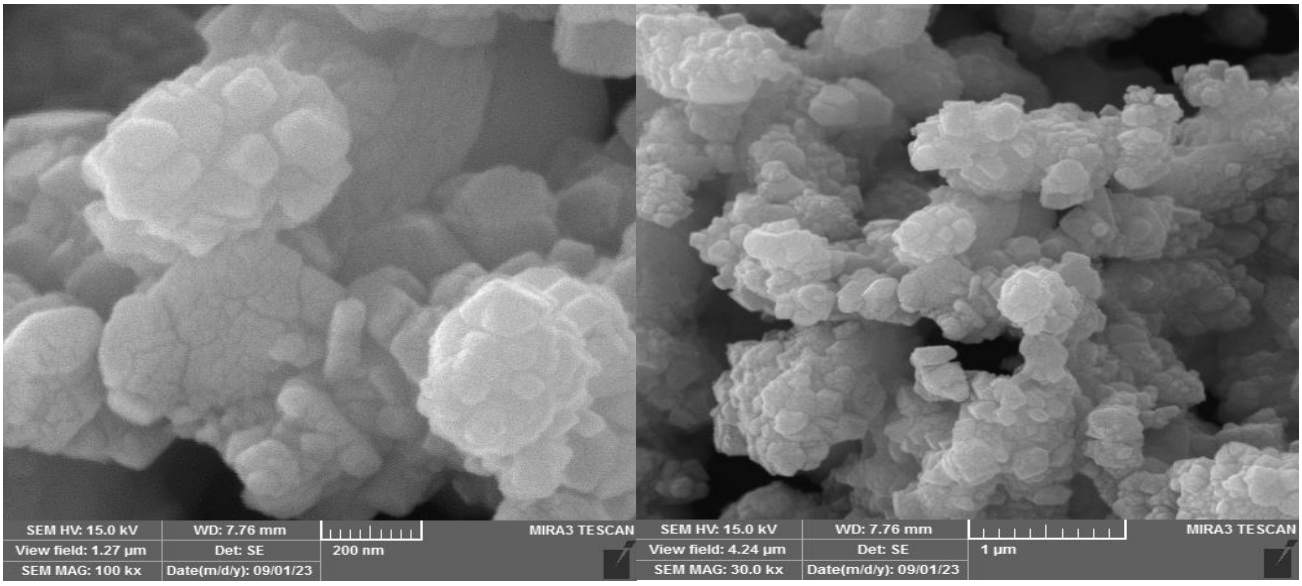

Figure 1: The SEM image for the CdO thin film deposited on the silicon substrate with two different magnifications.

Fig. 2 illustrates the experimental results obtained using AFM to analyze the surface morphology of the CdO thin film. The surface of the CdO thin film is characterized by a high density of regularly connected crystals, which exhibit no voids or holes. This structural configuration suggests that the CdO thin film possesses a high degree of homogeneity and crystalline regularity.

In contrast, PSi surface displayed a homogeneous, regular morphology with spherical pores. These pores are uniformly distributed and separated by nanoscale spaces, contributing to the overall regularity of the surface structure. Table 1 documented the morphological parameters for both CdO and PSi. The metrics such as surface roughness, pore size, and crystalline orientation provide a clearer understanding of the differences in surface characteristics between the two materials.

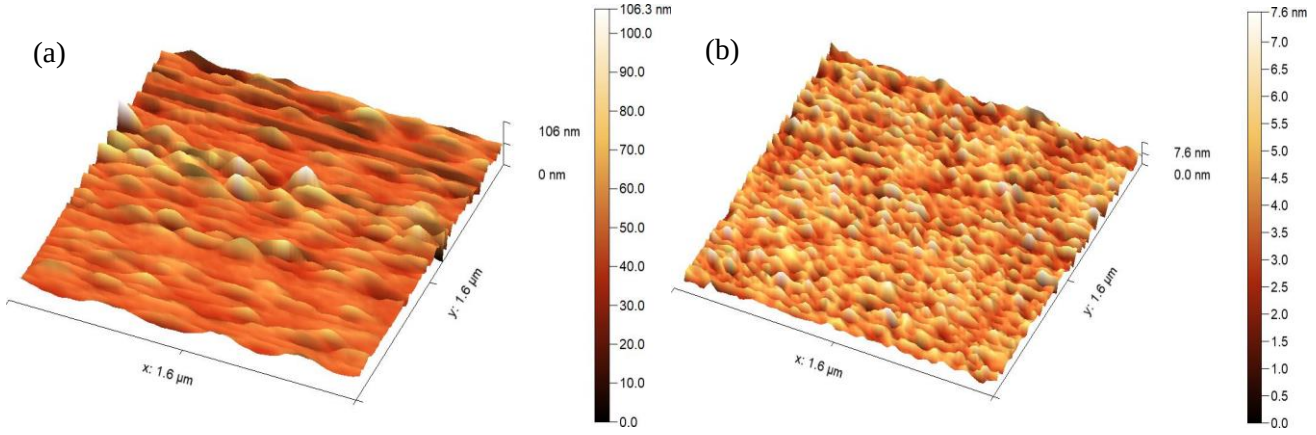

Figure 2: AFM images of (a) CdO film and (b) PSi/Si substrate.

Table 1: Average grain size, the root mean square, and the roughness average for the CdO and PSi.

Samples	Average grain size (nm)	Root mean square (nm)	Roughness average (nm)
CdO	7.20	1.24	0.96
Psi	63.82	9.03	5.87

X-ray diffraction was used to examine the structural features of CdO film and PSi. The XRD spectra displayed a distinct two-deflection peak. The first peak is a strong, sharp, and narrow single peak at $2\theta = 69.7°$ corresponding to the (400) orientation direction, which confirmed the cubic monocrystalline structure of the Si layer (according to ICDD). The second peak is at (61.98) as depicted in **Fig. 3**.

The results of XRD of crystalline silicon and PSi material showed that the c-Si peak exhibits higher intensity and expansion compared to the PSi peak, which might be attributed to ray diffraction of nano-sized crystals on the walls between pores, thus confirming the PSi layer maintains its crystalline form, but slightly shifted to a smaller diffraction angle [16]. The measured crystalline size of PSi by XRD was (61.18) nm, which was comparable with the value reported from the AFM image (63.82) nm.

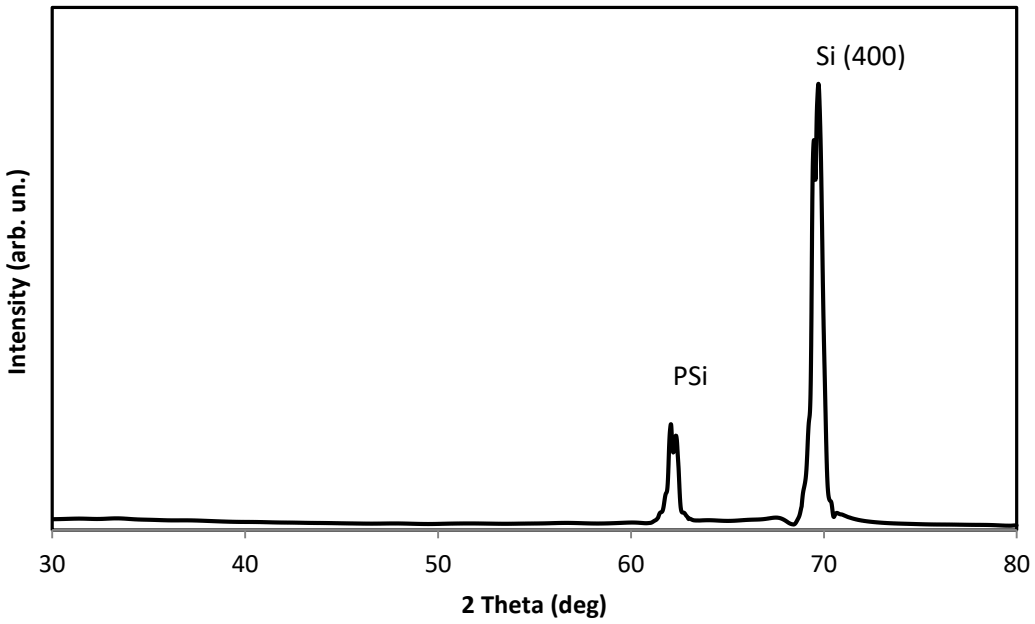

Figure 3: X-ray Diffraction pattern of the PSi / Si wafer.

The XRD diffraction pattern of synthesized CdO film deposited on quartz are shown in **Fig. 4**. The XRD patterns of CdO contain two prominent peaks at diffraction angles (31.17o) and (38.75o), corresponding to (002) and (111), respectively. No evidence of the cubic face matches the standard peaks at the planes (002) with Cd (Card No. 005-0640). The structural parameters of CdO listed in **Table 2** indicate that the grain size measurement of the prepared film was approximately 20 nm, higher than that obtained from the AFM result.

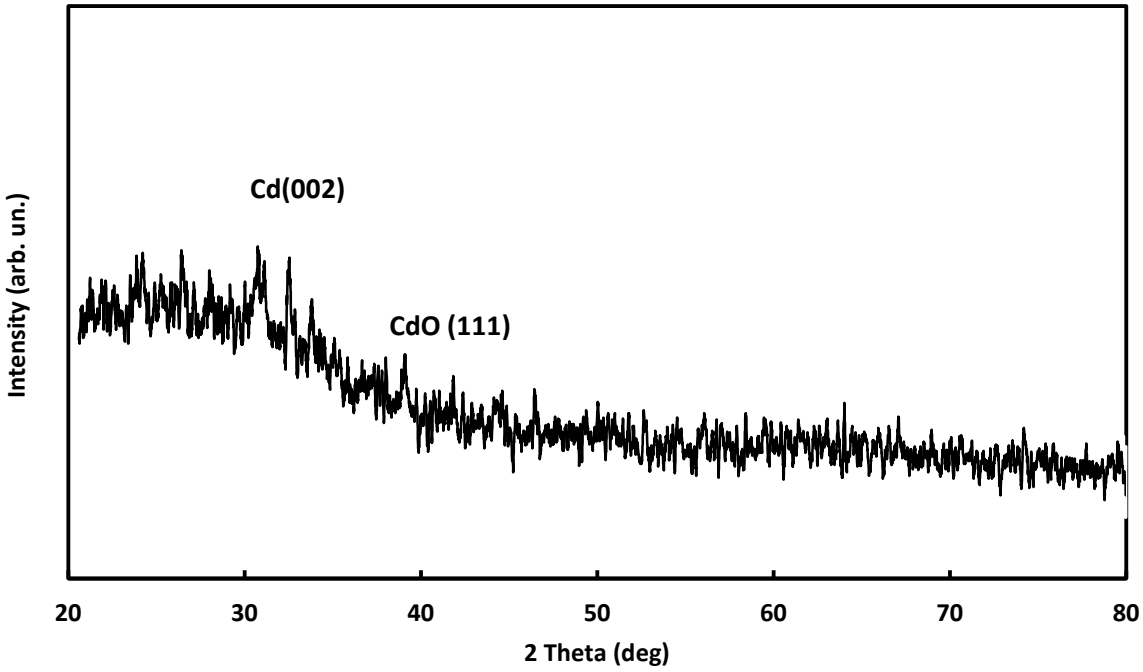

Figure 4: XRD for the CdO thin film deposited on the quartz substrate.

Table 2: The structural features of CdO obtained from the XRD test.

2Θ (deg)	hkl (plane)	d (Å)	FWHM (deg)	D (nm)	$\delta \times 10^{14}$ lines.m^{-2}	$\eta \times 10^{-4}$ lines^{-2}.m^{-4}
31.17	(002)	5.67	0.41	20.51	23.76	16.89
38.75	(111)	4.59	0.52	16.75	35.60	20.67

Fig. 5a shows the absorption spectrum of the CdO thin film. The absorption value increased with the increase in wavelength, and its maximum value was recorded at 340 nm. Furthermore, its value declines rapidly, approaching 500nm, and then maintains a roughly constant level with a slight decrease as the wavelength increases. The wide absorption range extends from near ultraviolet to the visible range, making CdO suitable for use with the Si/PSi solar cell duo to increase its absorption spectrum, and improving its efficiency [15, 17]. The energy gap value was measured by extrapolating the straight part of the carve plotted between photon energy and the result of the photon energy square multiplied by absorption coefficient t factor 2 or 1/2, depending on the transition type [18]. As shown in **Fig. 5b**, the value of a direct band gap is 2.55 eV for the prepared CdO film. These results matched values obtained by other researchers [19]. The correlation between the extinction coefficient (K), optical conductivity (σ), and photo wavelength is presented in **Fig. 6**. The CdO thin films have a higher light absorption capacity compared to previous studies utilizing different techniques [20]. The films were capable of absorbing 46% more light in the UV range and 66% more light throughout the absorbance spectrum (Wadi 2017) conducted a study and revealed that the optical absorption of conventional films was 1.6, with an absorbance spectrum ranging from 380 to 500 nm. Although the absorption range did not change, the researcher observed a significant improvement of over 100% in the absorption value compared to previous results [21].

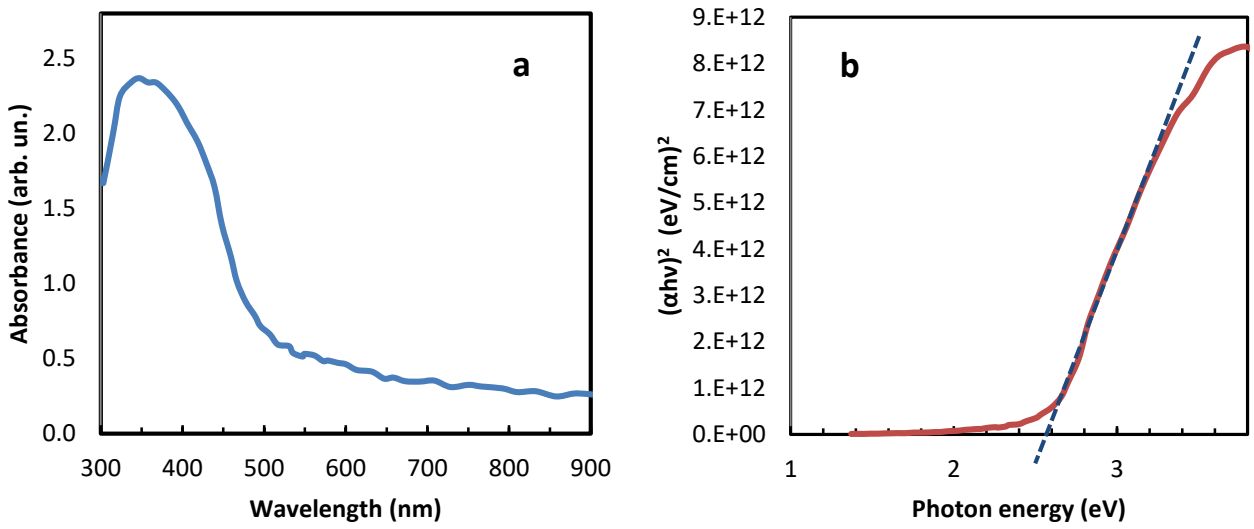

Figure 5: a) Optical absorbance of the CdO thin film deposited on the quartz substrate. **b**) Relation between $(\alpha h\nu)^2$ and photon energy.

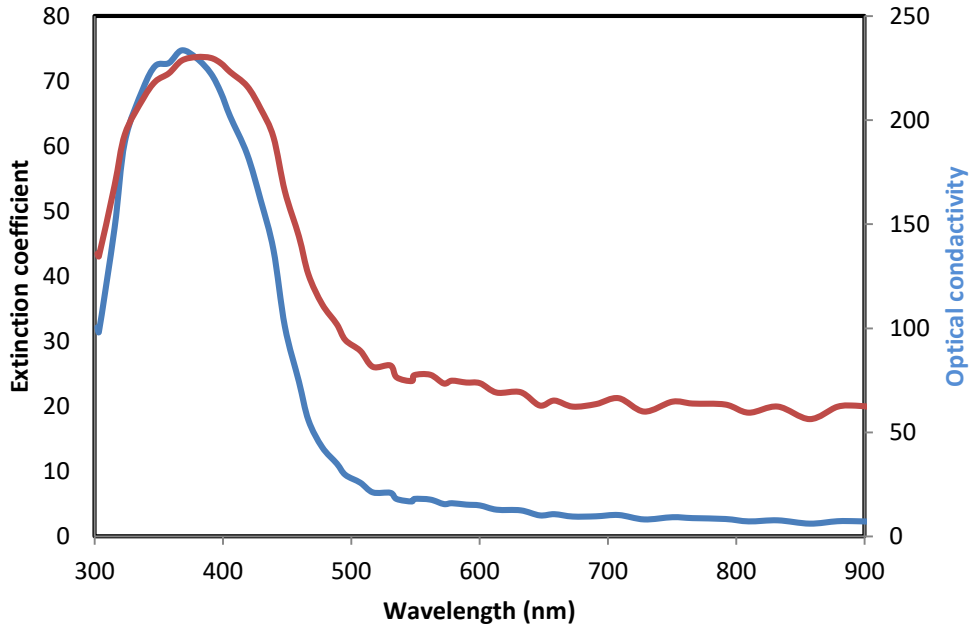

Figure 6: relation between Extinction coefficient, optical conductivity, and absorbed photon wavelength.

The photoluminescence spectra (P.L.) for the CdO/Psi/Si sample are shown in **Fig. 7.** It can be noticed that there are three distinguished peaks located at 1027, 700, and 530 nm, respectively. The peak of CdO appears at a wavelength of 530 nm with an energy gap of 2.67e.V. This result is lower than that extracted from UV-visible measurement 2.55 eV. This difference may be attributed to the difference in the measuring process; UV-visible spectroscopy requires more energy because it involves transferring electrons from the valence band to the conduction band. In addition, P.L. spectroscopy measures the energy of the emitted photon caused by the recombination process between the e-h pair, which typically involves a minor energy difference [18]. Meanwhile, the second and third peaks at 1.7 and 1.2 represent the value of PSi and silicon energy gap [20].

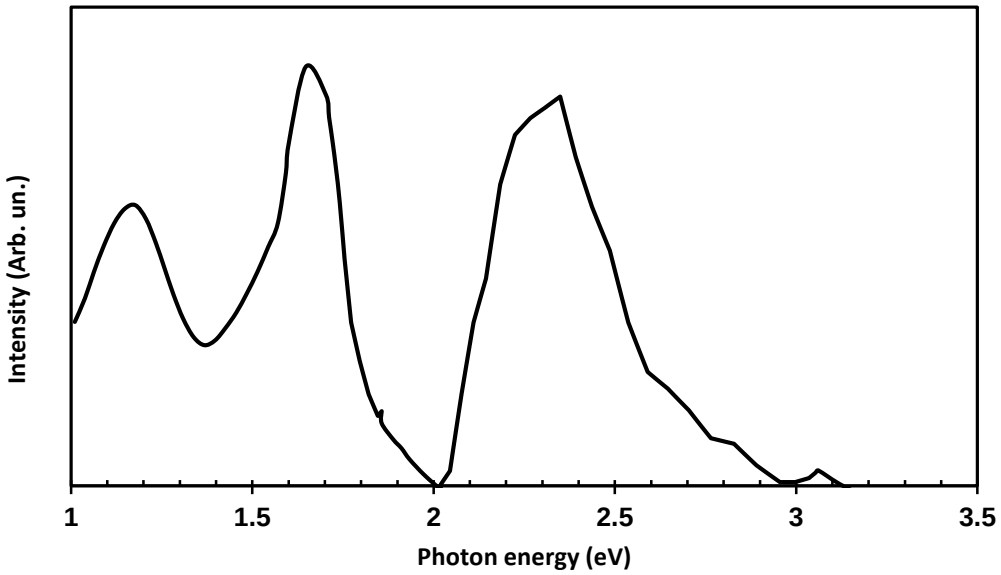

Figure 7: The photoluminescence spectra for the CdO/ Psi/Si.

The FTIR spectrum of CdO is displayed in **Fig. 8**. The FTIR spectrum confirms strong interactions between cadmium and oxygen at the wavelength 717 cm^{-1}. The metal-oxygen (MAO) bond was observed at 1200 cm^{-1}, which indicates the formation of CdO molecules. A wide band at 3421 cm^{-1} is caused by the O-H stretching of water molecules chemically associated with CdO. A strong band at 3421 cm^{-1} is assigned to the O-H stretching vibration of hydroxyl groups of CdO. Incorporating a nano-sized CdO matrix causes slight changes in the intensities of the absorption band at 1630 cm^{-1} and the formation of new absorption bands at 1031 cm^{-1}, which is attributed to the metal-oxygen stretching of CdO. The existence of nano-CdO in the oxygen matrix is confirmed by the peaks observed at 1630 cm^{-1}. Table 3 presents the data obtained from FTIR spectral analysis of the CdO thin films. It provides a concise summary of the determined wavenumbers, associated bond or vibration types, and their respective representations, as well as a concise overview of the significant interactions and structural elements detected in the spectrum.

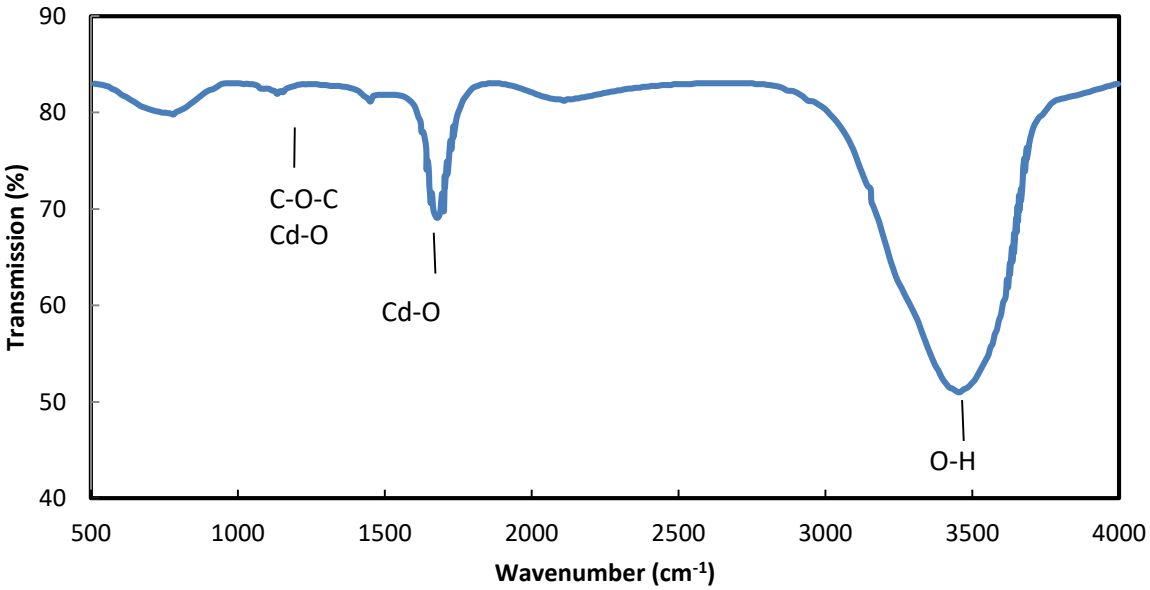

Figure 8: FTIR spectrum of CdO thin film.

Table 3: FTIR Spectral Analysis: Identified Bonds and Corresponding Vibrations in CdO Thin Film.

Representation	Bond/Vibration	Wavenumber (cm^{-1})
Strong interactions between cadmium and oxygen molecules	Cd-O interaction	717
Formation of CdO molecules	Metal-oxygen (MAO) bond	1200
Water molecules chemically associated with CdO	O-H stretching	3421
Hydroxyl groups of CdO	O-H stretching	3421
The presence of nano-CdO in the oxygen matrix peaks	Metal-oxygen stretching of CdO	1630
New absorption bands due to the incorporation of nano-sized CdO matrix	Metal-oxygen stretching of CdO	1031

Fig. 9 shows the FTIR for pours silicon and shows the appearance of several bonds that confirmed the formation of holes on the silicon to form the pours silicon, including a bond of Si-H within a wave number 1000-1500 cm^{-1} at the absorption beam 1663cm^{-1}. Also, the C-H bond is within 2500-3000cm^{-1} at the absorption beam 2857cm^{-1}, and the O-H bond is within a wave number 3000-3600cm^{-1} at the absorption beam 3428-3766cm^{-1}. Table 4 summarizes the results of the investigation of porous silicon by Fourier Transform Infrared (FTIR) spectral. The wavenumbers, bond or vibration types, and representations briefly describe the spectrum's major interactions and structural aspects.

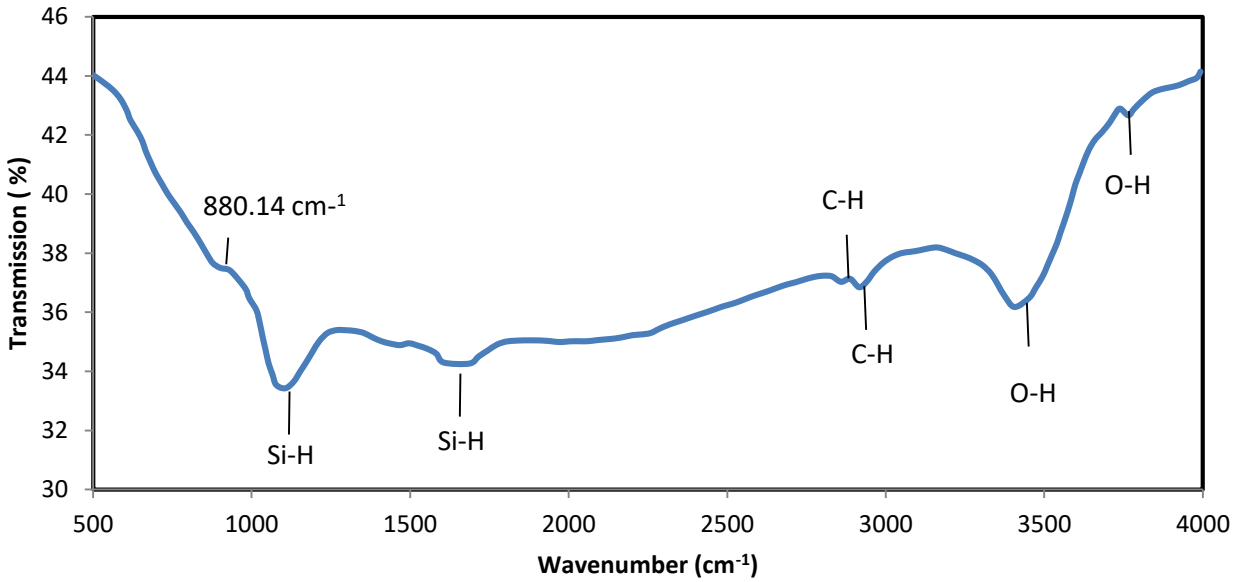

Figure 9: FTIR spectrum of the PSi

Table 4: Summary of FTIR Spectral Analysis of Porous Silicon.

Wavenumber (cm^{-1})	Bond/Vibration	Representation
1000-1500	Si-H bond	Confirmation of hole formation on silicon
1663	Si-H bond	Absorption peak indicating Si-H bond presence.
2500-3000	C-H bond	Absorption peak indicating C-H bond presence.
2857	C-H bond	Specific absorption peak for C-H bond
3000-3600	O-H bond	Broad absorption range indicating O-H bond presence
3428-3766	O-H bond	Specific absorption peaks indicating O-H bond presence

Fig. 10a shows the dark current as a function of the voltage for the forward and reverse biases. The dark current has a positive correlation with the voltage in both forward and reverse bias. There is an increase in the transfer of electrons from the valence band to the conduction band, and accordingly, the current increases due to the use of

porous silicon, which improves the material's properties, thus increasing absorption [21]. **Fig. 10b** shows the dark and illumination current of the prepared solar cell, and its characterization is presented in **Fig. 11**, showing it has a 15% fall factor and 0.16 efficiency.

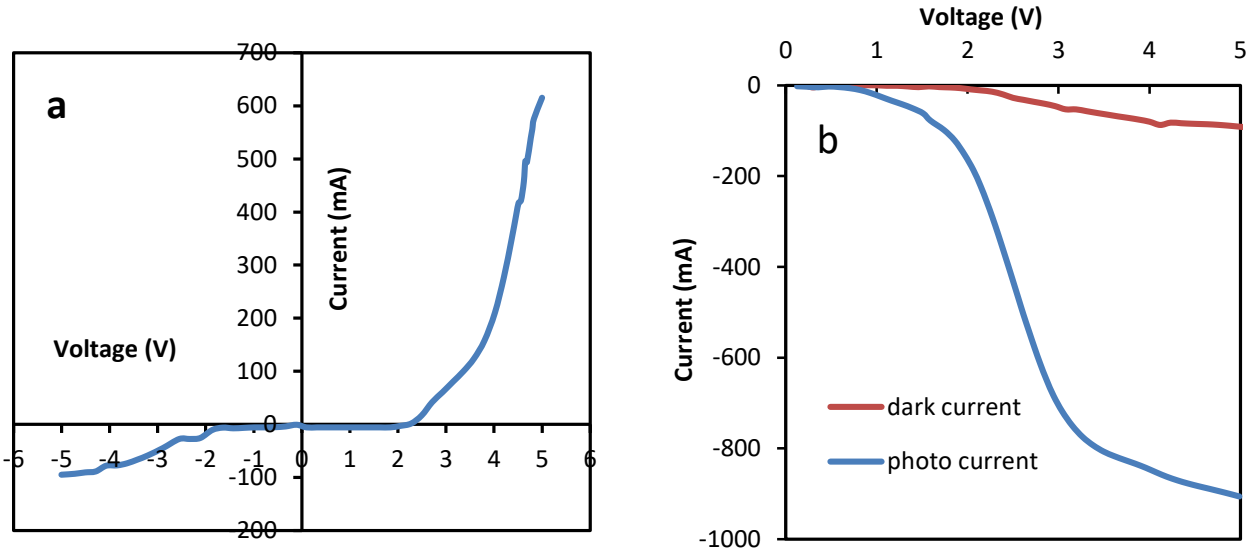

Figure 10: (a) forward and reverse bias current in the dark case. (b) dark and illumination current

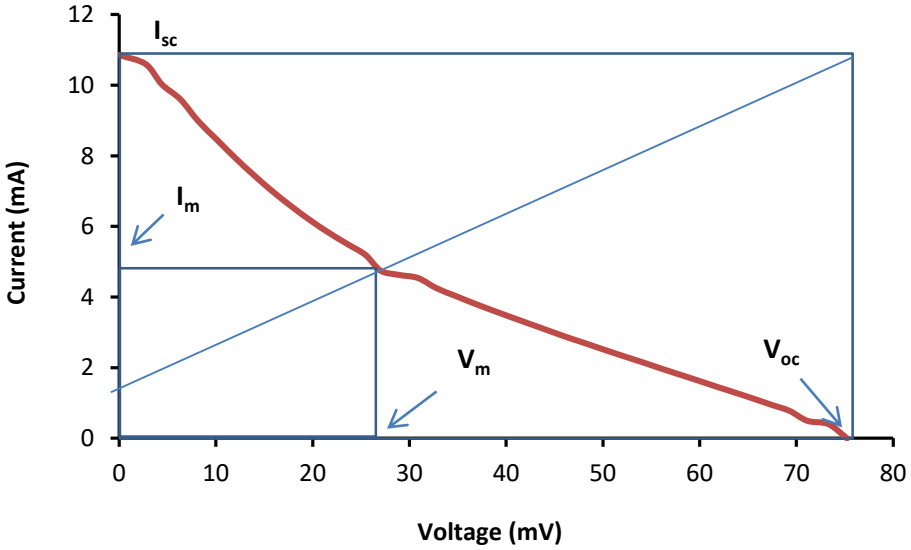

Figure 11: I-V characteristics of the fabricated CdO/Psi/Si solar cell

Based on the presented results of this study, it can be concluded that the study successfully synthesized CdO nanoparticles using pulsed laser ablation in liquid and deposited them onto PSi to create a solar cell. Characterization techniques such as SEM, AFM, XRD, and FTIR confirmed the formation and properties of the CdO film. The fabricated solar cell achieved an energy conversion efficiency of 0.16%.

SEM images of the CdO film on the PSi surface revealed variations in particle size. The CdO particles exhibited different sizes; the largest particles have a cubic form, and the smallest particles form clusters containing diffused particles within the porous silicon. These findings are in agreement with [21], which highlighted the heterogeneous nature of the CdO film on the PSi surface, indicating a range of particle sizes and structures within the material. In [22], the CdO films doped with aluminum (Al) exhibited homogeneous, smooth surfaces with a characteristic

spherical grain size. The roughness of the films, measured using root mean square (RMS), increased with higher Al dopant concentrations. These findings are consistent with the observations in the second study [23], where CdO films deposited on PSi substrates also showed homogeneous and smooth surfaces. Abed *et al*. [24] concentrate on investigating PSi surface modification for gas sensing applications. The authors incorporated pure SnO_2 nanoparticles and CuO-mixed SnO2 nanoparticles within a Psi layer to form SnO2: CuO/Psi nanocomposites. The Psi layer was prepared using a laser-assisted etching with a 40 mW/cm^2 laser illumination intensity. However, the two studies differed regarding the particle size and morphology of the CdO films on PSi surfaces. Shehab *et al*. [22] documented different sizes of CdO particles; the large particles were cubic, and the small particles formed clusters containing diffused particles within the porous silicon. This indicates the variations in particle distribution and morphology within the films. The presence of CuO nanoparticles had a substantial impact on the morphological characteristics of SnO_2 [23]. As the CuO content increases, SnO2 exhibits various morphologies, such as cubic and spherical shapes. By incorporating CuO nanoparticles in the Psi surface, it was possible to achieve nano architectures at the nanoscale. The CuO content significantly affected the plans, grain size, average surface roughness, homogeneity, and specific surface area of the SnO_2: CuO nanoparticle. The two previous studies reported the efficiency of solar cells, CdO performed as an efficient part of the optoelectronic device. According to Shehab *et al*. [22], Al-doped CdO films' structural and surface morphology properties were improved; hence, they have been used in many optoelectronic-related applications. The research study by Abdulridha *et al* directed attention to CdO films and demonstrated excellent sensitivity for the photo sensors' UV. Range [23]. The results revealed the benefits of CdO films on PSi surfaces because they elucidated the improvement in structural and morphological properties and their response to specific wavelengths of the devices, including solar cells and other optoelectronic devices, thus enabling high sensitivity. The AFM images indicated the differences in surface morphology structures of the CdO layer and PSi substrate. The CdO film surface exhibited a highly homogenous and crystalline structure. Here are a substantial number of consistently connected crystals, with no holes or voids present, whereas the PSi surface appeared uniform and regular with spherical spaces and gaps at nanoscale levels, In addition, the CNT was irregular, porous, and full of winding surfaces. These findings align with previous studies [25, 26], which suggest using CdO and SnO_2 films as alternative optical materials for solar cell purposes. The CdO films exhibited almost perfect uniformity and crystal periodicity. In contrast, the SnO_2 films were complete, adhered effectively, and displayed desirable properties for device applications, including structure, optical characteristics, and electrical behavior as well; as these features are crucial for solar panel operation because of their role in sunlight absorption, charge transportation and device performance. The CdO film has a high surface homogeneity and distinct crystalline structure. The film is made up of small strands of glass without any voids or holes. While the PSi surface is uniform and regular, a sphere with nanoscale gaps is uniquely characterized by the size of these spaces [26]. Based on the results, the DCO was covered by a nanostructure and homogenous composed nanowires with a diameter of less than 100 nm. The X-ray diffraction pattern of the spherical shape and the scanning electron microscope confirmed the existence of a cubic structure.

The results of X-ray diffraction analysis provide information about the crystal structure of the samples. The XRD spectra of the PSi/Si wafer exhibited a strong, sharp, and narrow peak at $2\theta = 69.7°$, corresponding to the (400) orientation direction, confirming the cubic monocrystalline structure of the Si layer. The PSi peak is slightly shifted to a smaller diffraction angle, indicating the presence of nano-sized crystals on the walls between pores. The XRD patterns of the CdO film on quartz displayed prominent peaks at $2\theta = 31.17°$ and 38.75°, corresponding to the (002) and (111) crystal planes, respectively, confirming the crystal structure of CdO. The optical properties of the CdO film are investigated through UV-visible spectroscopy and photoluminescence spectroscopy. The absorption spectrum of the CdO film showed an increase in absorption with wavelength decreasing, reaching a maximum value at 340 nm. The CdO film exhibited a wide absorption range extending from near ultraviolet to the visible range, making it ideal for enhancing the absorption spectrum of Si/PSi solar cells. The direct band gap energy of the CdO film was measured to be 2.55 eV.

The PSi was characterized by XRD, FTIR, and AFM. The FTIR analyzes showed that Si dangling bonds of the as-prepared PSi layer have a large amount of hydrogen, forming weak Si–H bonds. The structural, morphological, optical, and electrical properties of CuO NPs have been studied. X-ray diffraction measurement confirms that the CuO NPs were tetragonal crystal structures. AFM reveals that produced CuO NPs have a spherical shape. The

energy band gap of CuO NPs prepared was about (2.61eV). The effect of CuO NPs diffused on PSi hetero diode was reported. The findings are consistent with the literature [27, 28], supporting using CdO films and Psi structures to improve solar cell efficiency.

Our results indicated the characterization of CdO and PSi films using FTIR spectroscopy and their implications for solar cell performance. The FTIR spectra of CdO indicated the presence of Cd-O bonds and water molecules hydroxyl groups. The FTIR spectrum of PSi showed three bonds (i.e., Si-H, C-H, and O-H) related to the hole formation in Si. Observations of dark current reveal the electron transfer rate and charge carrier transportation during forward and reverse sweeps of applied voltage due to the presence of porous silicon. According to the literature, the experiments demonstrated the promising prospects of Psi for developing more efficient devices. Furthermore, the synthesis and identification of nanostructured silicon and CuO nanoparticles involve fabricating porous structure silicon hetero-diodes, which can be characterized using XRD and AFM techniques. Regarding solar cell performance, the information reported in the current study showed that incorporating PSi and CuO nanoparticles into PSi heterojunctions can be a promising technology with a high potential to boost the performance of solar cells. CuO nanoparticles, which may provide wide energy separation and other desirable optoelectronic properties, can be incorporated to increase the light absorption and charge carrier transport process.

4. Conclusions

The study has successfully achieved its objectives in producing CdO thin films using the PLD process and investigating their potential applications in the field of renewable energy. The results have significant implications for improving the efficiency of PSi solar cells. In addition, the research has demonstrated the improvement of the optical and electrical properties of CdO thin films, which have the potential to enable advances in the development and functionality of future solar systems. Subsequent research could improve the deposition parameters and investigate the incorporation of CdO thin films with other substances to utilize their capabilities in various renewable energy applications. The initial results of the PLA preparation process indicate that it is a promising technique for achieving high homogeneity with a particle size of 20 nm. The ultraviolet absorption properties of the material enhance the performance of silicon solar cells by expanding the range of light absorbed and efficiently converting it into electrical energy. High absorption was observed between 300 and 500 nm wavelength in the UV range. Further research is proposed to investigate the effects of heat treatment on the thin film produced at different heat treatment temperatures, which will improve the structural integrity and absorptivity of the material.

Conflict of Interest

The authors declare that they have no conflict of interest.

References

[1] J. A. Spencer, A. L. Mock, A. G. Jacobs, M. Schubert, Y. Zhang, and M. J. Tadjer, "A review of band structure and material properties of transparent conducting and semiconducting oxides: Ga_2O_3, Al_2O_3, In_2O_3, ZnO, SnO_2, CdO, NiO, CuO, and Sc_2O_3," *Appl. Phys. Rev.*, vol. 9, no. 1, 2022.

[2] J. R. Nolen, E. L. Runnerstrom, K. P. Kelley, T. S. Luk, T. G. Folland, A. Cleri, *et al.*, "Ultraviolet to far-infrared dielectric function of n-doped cadmium oxide thin films," *Phys. Rev. Mater.*, vol. 4, no. 2, p. 25202, 2020.

[3] I. Suhani, S. Sahab, V. Srivastava, and R. P. Singh, "Impact of cadmium pollution on food safety and human health," *Curr. Opin. Toxicol.*, vol. 27, pp. 1–7, 2021.

[4] M. B. A. Bashir, E. Y. Salih, A. H. Rajpar, G. Bahmanrokh, and M. F. M. Sabri, "The impact of laser energy on the photoresponsive characteristics of CdO/Si visible light photodetector," *J. Micromechanics Microengineering*, vol. 32, no. 8, p. 85006, 2022.

[5] E. T. Salim, R. A. Ismail, M. A. Fakhri, B. G. Rasheed, and Z. T. Salim, "Synthesis of cadmium oxide/Si heterostructure for two-band sensor application," *Iran. J. Sci. Technol. Trans. A Sci.*, vol. 43, no. 3, pp. 1337–1343, 2019.

[6] Z. Azam, A. Ayaz, M. Younas, Z. Qureshi, B. Arshad, W. Zaman, *et al.*, "Microbial synthesized cadmium oxide nanoparticles induce oxidative stress and protein leakage in bacterial cells," *Microb. Pathog.*, vol. 144, p. 104188, 2020.

[7] H. Soonmin, "A review of metal oxide thin films in solar cell applications," *Int. J. Thin Film Sci. Technol*, vol.

11, no. 1, 2022.
[8] Y. Wang, M. Li, B. Fan, Y. S. Wong, C. Y. Lo, C. K. G. Kwok *et al.*, "Flexibility of room-temperature-synthesized amorphous CdO-In_2O_3 alloy films and their application as transparent conductors in solar cells," *ACS Appl. Mater. Interfaces*, vol. 13, no. 36, pp. 43795–43805, 2021.
[9] Y. Wang, C. Y. Lo, Y. S. Wong, C. K. G. Kwok, S. K. Shil, and K. M. Yu, "Electrical conductivity and effects of mechanical bending of flexible amorphous transparent conducting CdO-Ga_2O_3 films synthesized by room temperature sputtering," *J. Alloys Compd.*, vol. 875, p. 160000, 2021.
[10] A. A. H. Ali, H. A. Noor, and S. A. Hussain, "Study of the effect of non-thermal plasma on the structural properties of pure Cadmium Oxide thin Films (CdO) prepared by Pulsed laser Deposition Technique (PLD)," *J. Kufa-Physics*, vol. 11, no. 1, pp. 63–70, 2019.
[11] T. S. Hussein and A. F. Ahmed, "Laser induced plasma of cadmium oxide: structural, morphological and optical properties," in *Journal of Physics: Conference Series*, IOP Publishing, 2021, p. 12012.
[12] G. K. Yogesh, S. Shukla, D. Sastikumar, and P. Koinkar, "Progress in pulsed laser ablation in liquid (PLAL) technique for the synthesis of carbon nanomaterials: a review," *Appl. Phys. A*, vol. 127, pp. 1–40, 2021.
[13] T. Gera, E. Nagy, T. Smausz, J. Budai, T. Ajtai, F. Kun-Szabó, *et al.*, "Application of pulsed laser ablation (PLA) for the size reduction of non-steroidal anti-inflammatory drugs (NSAIDs)," *Sci. Rep.*, vol. 10, no. 1, p. 15806, 2020.
[14] S. M. A. Al-Dujayli and N. A. Ali, "The effects of CuO doping on structural, electrical and optical properties of CdO thin films deposited by pulsed laser deposition technique," *J. OVONIC Res.*, vol. 18, no. 4, pp. 579–590, 2022.
[15] M. A. Abd, A. H. Ali, and A. N. Abd, "synthesis and investigation of CdO NPs for solar cell applications," *Mustansiriyah J. Sci. Educ.*, vol. 20, no. 5, pp. 1–12, 2019.
[16] B. Al-Jumaili, Z. A. Talib, A. Ramizy, A. I. Aljameel, H. Baqiah, N. M. Ahmed, *et al.*, "Formation and photoluminescence properties OF porous silicon/copper oxide nanocomposites fabricated via electrochemical deposition technique for photodetector application," *Dig. J. Nanomater. Biostructures*, vol. 16, no. 1, pp. 297–310, 2021.
[17] H. I. Hussein, A. H. Shaban, and I. H. Khudayer, "Enhancements of p-Si/CdO thin films solar cells with doping (Sb, Sn, Se)," *Energy Procedia*, vol. 157, pp. 150–157, 2019.
[18] R. Karoui, "Spectroscopic technique: fluorescence and ultraviolet-visible (UV-Vis) spectroscopies," in *Modern techniques for food authentication*, Elsevier, 2018, pp. 219–252.
[19] T. Prakash, E. R. Kumar, G. Neri, T. M. Bawazeer, K. Alkhamis, A. Munshi, *et al.*, "Evaluation of structural, morphological and optical properties of CdO nanostructures," *Ceram. Int.*, vol. 48, no. 1, pp. 1223–1229, 2022.
[20] B. Gelloz, "Photoluminescence of porous silicon," *Handb. Porous Silicon*, pp. 307–320, 2014.
[21] T. Tieu, M. Alba, R. Elnathan, A. Cifuentes-Rius, and N. H. Voelcker, "Advances in porous silicon–based nanomaterials for diagnostic and therapeutic applications," *Adv. Ther.*, vol. 2, no. 1, p. 1800095, 2019.
[22] S. Banerjee, C. Prabhakar, P. C. Chakraborti, and S. K. Saha, "Image processing based automated solution for analysis of dimple fracture surfaces," *Eng. Res. Express*, vol. 2, no. 4, p. 45029, 2020.
[23] S. A. Abdulridha, I. M. Ali, and A. A. Shihab, "Effect of thickness variation CdO/PSi thin films on detection of radiation," in *AIP Conference Proceedings*, AIP Publishing, 2019.
[24] H. R. Abed, A. M. Alwan, A. A. Yousif, and N. F. Habubi, "Efficient SnO2/CuO/porous silicon nanocomposites structure for NH3 gas sensing by incorporating CuO nanoparticles," *Opt. Quantum Electron.*, vol. 51, no. 10, p. 333, 2019.
[25] A. Abdelkrim, S. Rahmane, O. Abdelouahab, A. Hafida, and K. Nabila, "Optoelectronic properties of SnO_2 thin films sprayed at different deposition times," *Chinese Phys. B*, vol. 25, no. 4, p. 46801, 2016.
[26] R. A. Ismail, A.-M. E. Al-Samarai, S. J. Mohmed, and H. H. Ahmed, "Characteristics of nanostructured CdO/Si heterojunction photodetector synthesized by CBD," *Solid. State. Electron.*, vol. 82, pp. 115–121, 2013.
[27] K. Omar and K. A. Salman, "Porous Silicon Solar cell with anti-reflection coating layer for efficiency improved," *PONTE Int. Sci. Res. J.*, vol. 72, no. 5, 2016.
[28] K. A. Salman, Z. Hassan, and K. Omar, "Effect of silicon porosity on solar cell efficiency," *Int. J. Electrochem. Sci.*, vol. 7, no. 1, pp. 376–386, 2012.